2,4,6-Trisubstituted Pyrimidines as a New Class of Selective Adenosine A₁ Receptor Antagonists

Lisa C. W. Chang, Ronald F. Spanjersberg, Jacobien K. von Frijtag Drabbe Künzel, Thea Mulder-Krieger, Gijs van den Hout, Margot W. Beukers, Johannes Brussee, and Adriaan P. IJzerman*

Division of Medicinal Chemistry, Leiden/Amsterdam Center for Drug Research, P.O. Box 9502, 2300 RA Leiden, The Netherlands

Adenosine receptor antagonists usually possess a bi- or tricyclic heteroaromatic structure at their core with varying substitution patterns to achieve selectivity and/or greater affinity. Taking into account molecular modeling results from a series of potent adenosine A₁ receptor antagonists, a pharmacophore was derived from which we show that a monocyclic core can be equally effective. To achieve a compound that may act at the CNS we propose imposing a restriction related to its polar surface area (PSA). In consequence, we have synthesized two novel series of pyrimidines, possessing good potency at the adenosine A₁ receptor and desirable PSA values. In particular, compound **30** (LUF 5735) displays excellent A₁ affinity ($K_i = 4$ nM) and selectivity (≤50% displacement of 1 μM concentrations of the radioligand at the other three adenosine receptors) and has a PSA value of 53 Å².

Introduction

Adenosine is an endogenous ligand, ubiquitous throughout the human body. Its many extracellular functions are mostly accomplished through G protein coupled receptors, of which thus far four groups have been cloned and identified, the A₁, A₂A, A₂B, and A₃.[1] These adenosine receptors are present in varying levels of expression in different parts of the body. The widespread purpose and presence of adenosine has led to substantial research into the individual adenosine receptors as pharmaceutical targets. Over the years there have been many attempts to design and develop adenosine receptor antagonists, and over the past decade the search for ligands that show selectivity toward individual receptors has intensified as the role of the receptors in many therapeutic areas expands.[1] Xanthines were the first class of adenosine antagonists to be investigated and, as such, are also the most well explored. The best known compounds of this series are theophylline and caffeine (Figure 1). Research into nonxanthine ligands has grown tremendously in recent years, and the past decade has seen a number of new and interesting compounds showing varying degrees of selectivity for the adenosine receptors. In the early 1990s a paper by van Galen et al. detailed a model for the adenosine A₁ receptor binding site based on the superimposition of xanthines with adenosine.[2] A number of different computational-based papers for the A₁ receptor followed,[3−5] providing yet more models for the supposed binding site of the A₁ receptor. The consequential expansion in the field of adenosine A₁ antagonism generated a number of bi- and tricyclic heteroaromatic systems, featuring 2-nitrogen bicyclic systems (e.g., the naphthyridines),[6] 3-nitrogen bicyclic systems (e.g., deazaadenines),[7] 4-nitrogen bicyclic systems (e.g.,
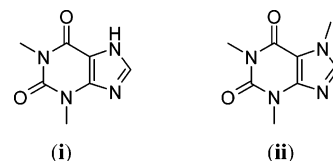

Figure 1. (i) Theophylline. (ii) Caffeine.

the pyrazolopyrimidines),[8] 3-nitrogen tricyclic systems (e.g., the imidazoquinolines),[9] and 4-nitrogen tricyclic systems (e.g., triazoloquinoxalines),[10] to name but a few groups. Indeed in two recent reviews[11,12] it is stated quite clearly that the different structural classes for A₁ adenosine receptor antagonists are bi-and tricyclic heterocyclic compounds. Moreover, an investigation in our group highlighted the general low affinity of monocyclic compounds.[13] The exceptions to this were two 5-membered heterocycles, namely, thiazoles and thiadiazoles.[13,14] In the wider field of adenosine receptor ligands, (dihydro)pyridines have been developed and explored as A₃ receptor antagonists by Jacobson et al.[15−17] and as adenosine receptor agonists by Bayer.[18] Although these series show affinity for the A₁ receptor, they have not been specifically investigated for A₁ receptor efficacy, and in some cases they have been developed to show particularly good, although not selective, affinity for the A₂B receptor.[19]

Adenosine A₁ receptors are in abundance in the mammalian brain, and the role that they play in important functions, such as in the modulation of neurotransmitter release, sleep regulation, and cognition enhancement, has been thoroughly investigated.[20−22] For this reason it is essential that a compound targeted at these therapeutic areas is able to cross the blood−brain barrier (BBB). Research into the BBB and the ability of a compound to cross it has become a highly investigated topic in recent years. A recent review[23] highlighted some "rules of thumb" which have emerged from numerous research articles from the past few

* To whom correspondence should be addressed. E-mail: ijzerman@lacdr.leidenuniv.nl. Tel: +31 (0)71 527 4651. Fax: +31 (0)71 527 4565.
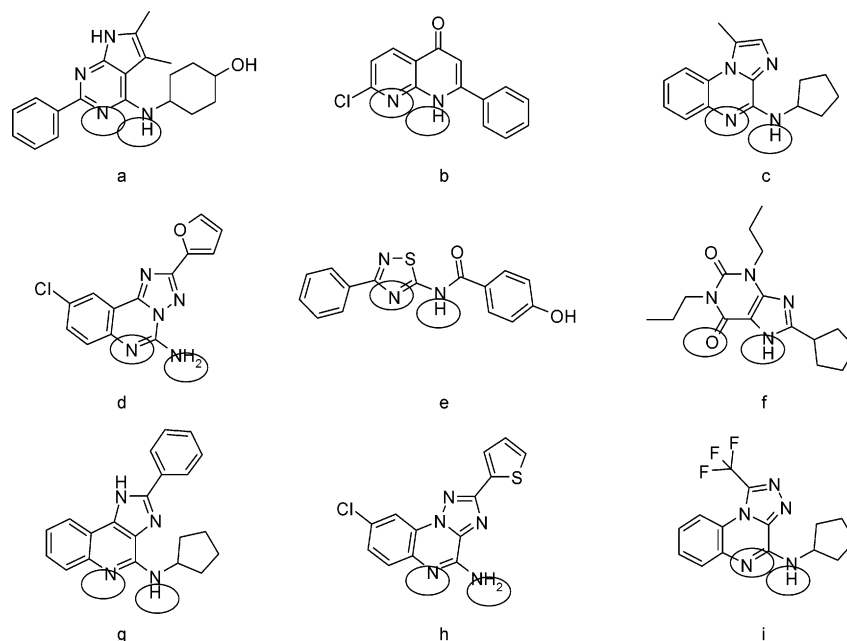
Figure 2. The nine A_1 adenosine receptor antagonists modeled in this study. Of the two areas marked on each molecule, the left ellipse signifies electron-poor regions corresponding to hydrogen-bond donating regions. The area marked with the right-hand ellipse on each molecule depicts electronically rich regions corresponding to hydrogen-bond accepting regions: **a** (K_i (hA$_1$) = 25 nM);[46] **b** (K_i (bA$_1$) = 0.15 nM);[6] **c** (K_i (rA$_1$) = 7.9 nM);[40] **d** (K_i (rA$_1$) = 21 nM; K_i (hA$_1$) = 3.5 nM;[47,48] **e** (K_i (rA$_1$) = 7.3 nM;[14] **f** (K_i (hA$_1$) = 3.9 nM);[48] **g** (K_i (rA$_1$) = 10 nM);[9] **h** (IC$_{50}$ (rA$_1$) = 28 nM);[10] **i** (K_i (rA$_1$) = 7.3 nM.[41]

years. Among these was the almost qualitative example that the sum of the nitrogen and oxygen atoms in a molecule should be five or less for that molecule to have a high chance of entering the brain.[24] Of the more quantitative prediction techniques, the rule that for good brain permeation, as for good intestinal absorption, the polar surface area (PSA) of a molecule should be below a certain limit has been very thoroughly investigated.[25−29] The PSA is defined as the surface area of a molecule occupied by nitrogen and oxygen atoms, and hydrogen atoms that are attached to these atoms.[29] It has become one of the most convenient and reliable parameters to calculate, and the limits for brain penetration according to research, e.g., by Kelder et al.,[25] have been proposed to be in the region of 60−70 Å^2.

In this present study, we subjected known ligands to molecular modeling investigations and derived a pharmacophore upon which we could design potent adenosine A_1 receptor antagonists. We describe the development of a series of novel mono-heterocyclic compounds that show high affinity for the human A_1 adenosine receptor, namely, the 2,6-diphenyl-4-amidopyrimidines. With the notion of the importance of the BBB, we also calculated PSA values on this set of compounds and realized that they were within the limits described by Kelder et al.[25] In consequence, we subsequently synthesized a second series of pyrimidines also with "good" PSA values. These 4,6-diphenyl-2-amidopyrimidines displayed equal affinity and a notable increase in selectivity for the A_1 adenosine receptor over the A_{2A} and A_3 receptors.

Results and Discussion

Molecular Modeling. Molecular modeling work was conducted on a number of ligands with high affinity and selectivity for the A_1 adenosine receptor as listed in Figure 2. The molecules were drawn in the SPARTAN[30]

molecular modeling package and minimized, and only the lowest energy conformer was taken into consideration. This conformer was then subjected to surface calculations, from which an electrostatic potential energy was drawn, and upon which the electron density was mapped; an example for DPCPX is given in Figure 3. In Figure 3, the shades of red and blue denote relatively electronegative and electron-poor regions, respectively. These areas are mapped upon the selection of compounds modeled. It can clearly be seen that all molecules have in common an adjacent electron-rich and -poor area at the "bottom" corresponding to hydrogen-bond accepting and donating regions, as denoted by the respective ellipses marked in Figure 2. Superimposition of the compounds using these regions as a basis resulted in the illustration seen in Figure 4. A simplified version is shown in Figure 5, where four of the antagonists of Figure 2 (**b**, **d**, **e**, **f**,) with the electrostatic potential energy surface of just one of the molecular models (**d**) were chosen to show the general pattern of the resulting superimposition. This resulting pharmacophore derived from the molecular modeling is illustrated with a schematic diagram in Figure 6. There seems to be a requirement for neighboring electronically rich and poor regions at the "bottom" of the molecule (labeled regions A and B) corresponding to hydrogen-bond accepting and donating regions, respectively. At the "top" of the figure (region C) there is a requirement for another hydrogen-bond acceptor. Furthermore, three lipophilic entities about the central core, labeled L_1, L_2, and L_3, are desirable for good binding properties.

This phamacophore is in agreement with a model for the bovine A_1 adenosine receptors as published by Da Settimo et al. to rationalize the SARs of a set of aryl-triazino-benzimidazolones.[31] This model was further exploited by the same group to provide a series of imidazotriazines with good affinity for the bovine A_1
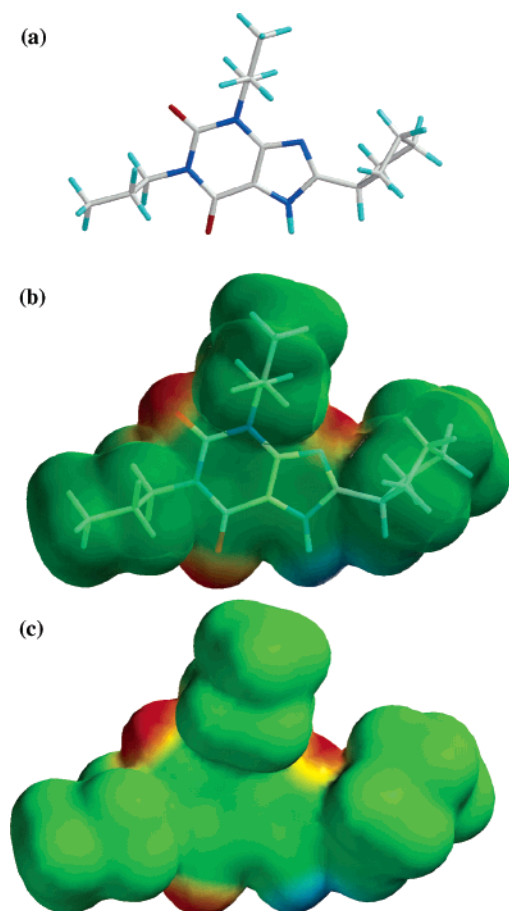
Figure 3. (a) DPCPX in its lowest energy conformer as calculated with Spartan. (b) DPCPX with the electrostatic potential energy surface mapped as a transparent cloud around the "stick" model. (c) Molecular electrostatic potential energy surface of DPCPX, where the color coding is in the range from −60 (deepest red) to 60 (deepest blue) kcal·mol⁻¹.
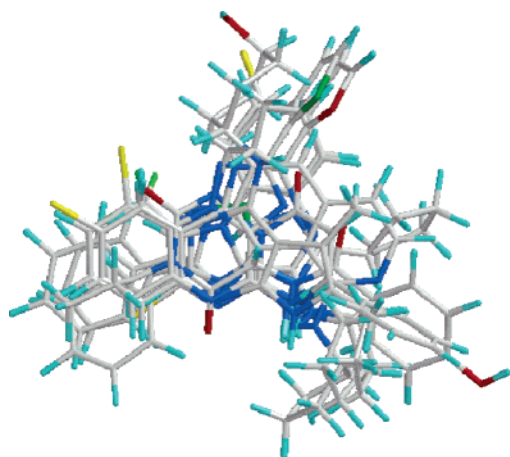

Figure 4. All nine molecules superimposed upon each other upon the hydrogen-bond donating and accepting regions, as seen marked in Figure 2.

receptor.[32] In 2002, Bondavalli and co-workers[33] carried out some computational work on a collection of eleven different A₁ antagonists using different methods to achieve a pharmacophore similar to that of Da Settimo et al. These models, however, were all based on bi- and tricyclic heteroaromatic cores, fueling new antagonists which were again bicyclic—the pyrazolopyridines of Bondavalli—or tricyclic—the triazinobenzimidazoles by
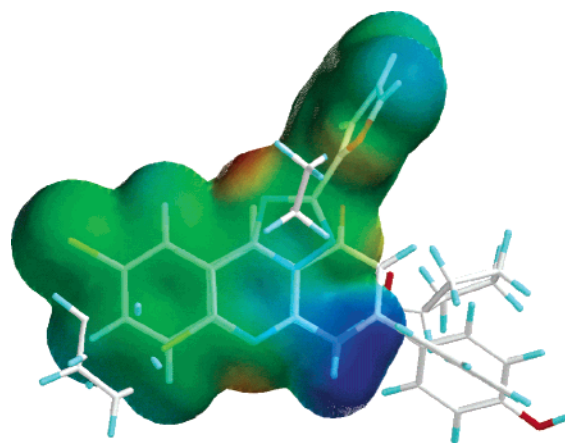
Figure 5. A simplified picture showing only four of the antagonists (**b, d, e, f**) superimposed upon each other, including the electrostatic potential energy surface of the antagonist **d**.
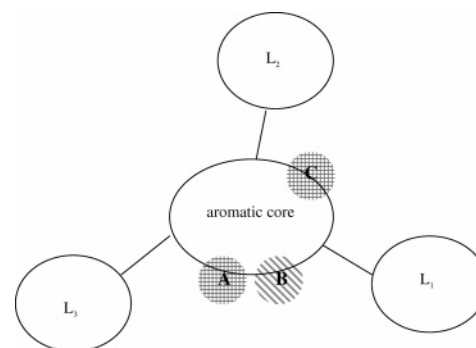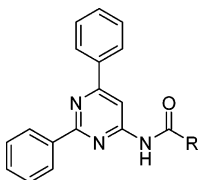

Figure 6. Schematic diagram of the resulting pharmacophore attained from the modeling study. A and B respectively represent H-bond accepting and donating regions at the "bottom" of the molecule. An H-bond acceptor is denoted by C. Three lipophilic domains are represented by L₁, L₂, and L₃.

Da Settimo. In our case, the model proposed only suggests an aromatic core with the given characteristics, to be substituted accordingly to fill the lipophilic pockets. Thus, it seemed that to fulfill the requirements of this model, a mono-heterocycle as the central core would be sufficient. Examining the model in more detail, a single aromatic group containing a nitrogen atom would fit the hydrogen-bond accepting region. An amido group in an adjacent position would fulfill hydrogen-bond donating and accepting regions B and C. The two lipophilic pockets L₂ and L₃ could be "filled" with phenyl groups to give an almost symmetric core, leaving the pocket L₁ to be explored thoroughly. Thus the 2,6-diphenyl-4-amidopyrimidines were conceived.

Polar Surface Area Calculations. The polar surface areas (PSA) of the molecules were calculated using Spartan 5.0 for SGI,[30] in combination with an in-house developed application called PolSurf 1.0. [A copy of PolSurf and its (C) source code can be obtained via the author.] First Spartan was used to build the molecule, optimize its 3D structure, and calculate its property data; subsequently PolSurf was applied to convert the raw data from the Spartan "input" and "proparc" files into the polar surface area of the molecule. The resulting PSA values were compared with data already available in the literature for calculations based on a single conformer and based upon van der Waals surface areas

Table 1. Affinities and PSA Values of the 2,6-Diphenyl-4-amidopyrimidines **4−20** in Radioligand Binding Assays at the Human Adenosine Receptors

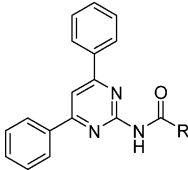| compd	R	calcd PSA values (Å^2)	hA$_1$[b]	hA$_{2A}$[c]	hA$_{2B}$[d]	hA$_3$[e]
				K_i (nM) or % displacement[a]		
4	Ph	50	671 ± 110	17%		1300 ± 300
5	4-Cl-Ph	50	35%	0%		33%
6	4-MeO-Ph	61	30%	0%		1170 ± 150
7	Me	52	37.5 ± 8.1	489 ± 140		6.88 ± 1.9
8	Et	51	9.50 ± 4.6	81.9 ± 14		22.4 ± 8.9
9	Pr	51	17.6 ± 5.3	124 ± 17		167 ± 51
10	Bu	51	109 ± 15	48%		392 ± 65
11	i-Pr	51	11.1 ± 6.2	376 ± 76		267 ± 39
12	CH$_2$CHMe$_2$	51	14.8 ± 2.7	157 ± 42		447 ± 62
13	CHEt$_2$	50	6.35 ± 0.4	381 ± 33	72%	57%
14 (LUF 5767)	CH(Me)(Et)	51	2.22 ± 1.1	899 ± 130	44%	147 ± 22
15	t-Bu	49	27.7 ± 6.2	18%		49%
16 (LUF 5764)	CH$_2$CMe$_3$	51	8.75 ± 4.1	32%	4%	39%
17	c-Pr	52	7.58 ± 1.3	189 ± 44		25.0 ± 2.4
18	c-Bu	51	6.49 ± 2.2	179 ± 58	74%	178 ± 57
19 (LUF 5740)	c-Pent	51	2.14 ± 0.1	196 ± 66	52%	170 ± 60
20	c-Hex	51	15.5 ± 8.4	208 ± 77		32%

[a] $K_i \pm$ SEM ($n = 3$), % displacement ($n = 2$). [b] Displacement of specific [^{3}H]DPCPX binding in CHO cell membranes expressing human adenosine A$_1$ receptors or % displacement of specific binding at 1 μM concentrations. [c] Displacement of specific [^{3}H]ZM241385 binding in HEK 293 cell membranes expressing human adenosine A$_{2A}$ receptors or % displacement of specific binding at 1 μM concentrations. [d] % Displacement of specific [^{3}H]MRS1754 binding in CHO cell membranes stably transfected with the human adenosine A$_{2B}$ receptor at 1 μM concentrations. [e] Displacement of specific [^{125}I]AB-MECA binding in HEK 293 cell membranes expressing human adenosine A$_3$ receptors or % displacement of specific binding at 1 μM concentrations.

as described by Clark.[27,28] We observed a highly significant correlation for the 75 compounds investigated (R^2 = 0.98, see Supporting Information for more details). Clark compared his calculated PSA values to experimental percentage fractional absorption data[27,28] and the "rule-of-five".[34] In consequence, he concluded that poor passive intestinal absorption occurred when a molecule has a PSA value of $\geq$ 140 Å^2. Likewise, Kelder et al.[25] published a similar paper stating that orally active drugs, when transported passively, should not exceed a PSA of 120 Å^2. Furthermore, the Kelder investigation also studied BBB penetration and concluded that, by decreasing the PSA to 60−70 Å^2, brain penetration could be achieved. As in our calculations, both parties use van der Waal surface areas, and only consider the heteroatoms N and O and any hydrogens that may be attached to them. We therefore propose the significant value of 60−70 Å^2 as the limit for PSA for brain penetration as suggested by Kelder et al.[25] as also relevant in this paper.

The PSA values of our initial series (the 2,6-diphenyl-4-amidopyrimidines) were calculated to be under the set limit, with a range of 49 (R = ^{t}Bu) to 61 (R = 4-MeOPh) Å^2. With reference to this series, a second set of ligands (4,6-diphenyl-2-amidopyrimidines) was designed with the pharmacophore and PSA limits in mind. Again, the hydrogen-bond accepting and donating regions are fulfilled by the nitrogen in the pyrimidine ring and the amido hydrogen, and again the carbonyl oxygen accounts for the hydrogen-bond accepting region at the "top" of the space. With only three nitrogen atoms, one oxygen atom, and one polar hydrogen atom, the PSA values (Table 2) were calculated to be within the

proposed 60−70 Å^2 limit. The two lipophilic areas labeled L$_2$ and L$_3$ were "filled" with aromatic phenyl groups and the third, labeled L$_1$, was again left to be explored.

Chemistry. The synthetic route to the 2,6-diphenyl-4-amidopyrimidines (**4−20**) is depicted in Scheme 1. The pyrimidinone ring was created by the reaction of the commercially available β-ketoester, ethyl benzoate, with benzamidine hydrochloride in the presence of a base to give the pyrimidinone ring (**1**). The first attempts to achieve the condensation using sodium ethoxide rendered only poor yields; changing the base to sodium hydroxide in accordance to a script by de Valk and van der Plas[35] improved the reaction significantly resulting, in a yield of 59%. Displacement of the hydroxide function was achieved with an excess of phosphoryl chloride containing phosphorous pentachloride, according to a preparation by Brown et al.[36] Subsequent substitution with ammonia in a sealed vessel gave the key 4-amino-2,6-diphenyl pyrimidinyl intermediate (**3**) in very good yields. The final step to give compounds **4−20** involved the formation of the amide bond. Attempts using the carboxylic acid with standard coupling agents, for example 1-(3-dimethylaminopropyl)-3-ethylcarbodiimide hydrochloride (EDC) and 1-hydroxybenzotriazole (HOBt), gave poor or no yields. As an alternative the amine was reacted with acid chlorides in the presence of triethylamine to give, in general, good to excellent yields. The pyrimidines **22−40** were synthesized according to the route depicted in Scheme 2. Guanidine was freed from its hydrochloride salt form with NaOH$_{(aq)}$ and reacted with benzylideneacetophenone according to a method described by Al-Hajjar and

Table 2. Affinities and PSA Values of the 4,6-Diphenyl-substituted-2-amidopyrimidines **22**−**40** in Radioligand Binding Assays at the Human Adenosine Receptors

compd	R	calcd PSA values (Å²)	K_i (nM) or % displacement[a]			
			hA₁[b]	hA₂ₐ[c]	hA₂ᵦ[d]	hA₃[e]
22	Ph	53	309 ± 73	5%		38%
23	4-Cl-Ph	53	0%	0%		3280 ± 1700
24	4-MeO-Ph	64	31%	45%		41%
25	4-Me-Ph	53	37%	0%		13%
26	3,4-diCl-Ph	53	0%	0%		30%
27	3-Cl-Ph	53	368 ± 66	22%		41%
28	Me	53	483 ± 90	31%		237 ± 150
29	Et	53	46.4 ± 2.5	893 ± 160		547 ± 47
30 (LUF 5735)	Pr	53	3.70 ± 1.9	7%	54%	38%
31	Bu	53	27.6 ± 10	0%		23%
32	Pent	52	28%	0%		24%
33 (LUF 5737)	*i*-Pr	51	8.87 ± 4.2	44%	79%	45%
34	*t*-Bu	50	224 ± 120	0%		4%
35	CH₂CHMe₂	51	25.1 ± 6.6	42%		23%
36	CHEt₂	51	27.1 ± 5.7	11%		27%
37	c-Prop	52	24.9 ± 4.9	228 ± 95		676 ± 120
38	c-But	53	107 ± 36	33%		18%
39 (LUF 5751)	c-Pent	51	11.4 ± 2.4	11%	42%	39%
40	c-Hex	51	119 ± 42	31%		9%

[a] K_i ± SEM ($n = 3$), % displacement ($n = 2$). [b] Displacement of specific [³H]DPCPX binding in CHO cell membranes expressing human adenosine A₁ receptors or % displacement of specific binding at 1 μM concentrations. [c] Displacement of specific [³H]ZM241385 binding in HEK 293 cell membranes expressing human adenosine A₂ₐ receptors or % displacement of specific binding at 1 μM concentrations. [d] % Displacement of specific [³H]MRS1754 binding in CHO cell membranes stably transfected with the human adenosine A₂ᵦ receptor at 1 μM concentrations. [e] Displacement of specific [¹²⁵I]AB-MECA binding in HEK 293 cell membranes expressing human adenosine A₃ receptors or % displacement of specific binding at 1 μM concentrations.

Scheme 1. Synthetic Route to the 2,6-Diphenyl-substituted-4-amidopyrimidines **4**−**20**[a]
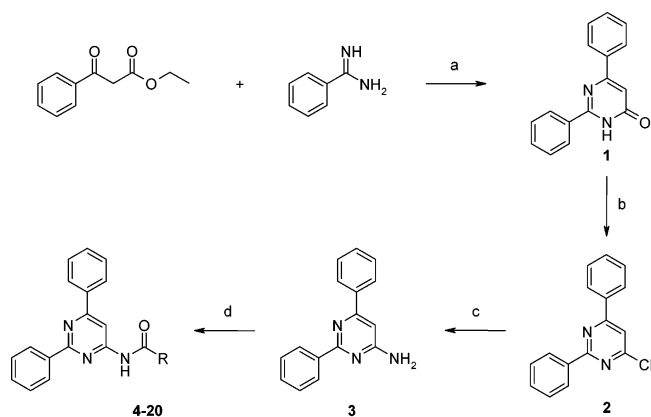

[a] (a) NaOH, EtOH; (b) POCl₃, PCl₅; (c) NH₃, EtOH; (d) RCOCl, Et₃N, 1,4-dioxane.

Sabri.[37] The amine was obtained in a 31% yield. This 2-aminopyrimidine (**21**) was then reacted with the respective acid chlorides in the presence of triethylamine to give the desired 2-amido compounds (**22**−**40**). These were obtained in 13−98% yields, where the reaction conditions for each substrate were not optimized.

Structure−Activity Relationships. The results of the binding assays for compounds **4**−**20** are represented in Table 1. There are distinct and vital differences in affinity for the compounds across the receptors, thus highlighting the variation in the electronic and spatial requirements necessary to create high affinity ligands

for the adenosine receptors. In consequence to previously published material in our group,[13,14,38] the first amides prepared were phenyl derivatives based on the Topliss[39] system of substitution, and assumed the L₁ pocket to be similar to L₂ and L₃ in size and shape. The initial compound (the unsubstituted phenyl derivative) shows fair affinity for the A₁ adenosine receptor at 670 nM with a 2-fold selectivity over the A₃ receptor (K_i = 1300 nM). Substituting following the Topliss system[39] gave little improvement in affinity, with only 4-methoxyphenyl derivative **6** showing a very slight gain in affinity at the A₃ receptor, in agreement with our previous publications.[13,38]

With the alkyl amides, significant improvements were made over the phenyl substituents at the L₁ pocket. In the straight-chained alkyls, from methyl to pentyl (**7**−**10**) a distinct optimum is apparent for a two-carbon chain (compound **8**) at the A₁ receptor, with an affinity of 9.5 nM. This pattern is repeated at the A₂ₐ receptor, with a K_i of 82 nM (**8**). At the A₃ receptor, however, the methyl substituted derivative (**7**), with an affinity of 7 nM, was far and away the better compound. In terms of selectivity, compound **7** was 5-fold more selective for the A₃ receptor than for the A₁ receptor, while, in a slight reversal of this, compound **8** showed a 2-fold selectivity in favor of the A₁ adenosine receptor over the A₃ receptor. Better selectivity for the A₁ adenosine receptor came with the *n*-propyl derivative (**9**) with an almost 7-fold better affinity over the A₂ₐ receptor (K_i = 17.6 nM vs K_1 = 124 nM) and by almost a factor of 10 with the A₃ adenosine receptor (K_i = 167 nM). From

Scheme 2. Synthetic Route to the 4,6-Diphenyl-substituted-2-amidopyrimidines **22−40**[a]
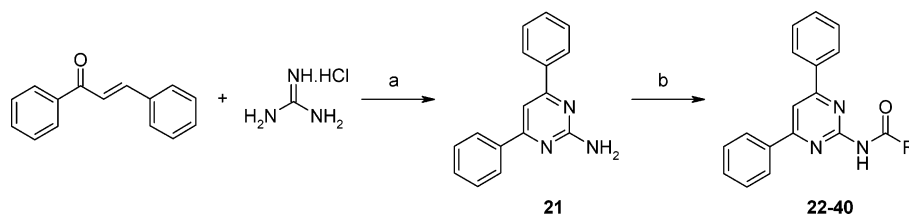
[a] (a) NaOH, EtOH, H_2O; (b) RCOCl, Et_3N, 1,4-dioxane.

these results, it seems that the lipophilic pocket (L_1) is not quite as "deep" for the A_1 adenosine receptor as expected.

To explore a "breadth" versus "depth" hypothesis of the L_1 pocket thrown up by the results of the straight-chained alkyls, a number of branched-alkyl derivatives (**11−15**) were made. Though all showed good to fair affinity across the adenosine receptors, the overall bias was toward the A_1 receptor. The isopropyl compound (**11**) showed a 24-fold selectivity for the A_1 receptor over the A_3 with an affinity of 11 nM vs 267 nM. Improving upon this, the isopentyl (**13**) showed a K_i value of 6 nM at the A_1 receptor, while losing a significant amount of affinity at the A_3 receptor. Compound **14** was overall the best of the branched alkyl group in terms of affinity to the A_1 receptor, with an affinity of 2.2 nM. The large, sterically hindered *tert*-butyl group seems to be tolerated only at the A_1 receptor, with compounds **15** and **16** showing little affinity for either the A_{2A} or the A_3 receptors, making these compounds highly selective for the A_1 adenosine receptor.

The cycloalkyl derivatives (**17−20**) were made to combine and confirm the length and breadth hypothesis of the L_1 pocket of the A_1 receptor drawn from the branched and straight alkyl derivatives. It is notable that the cyclopentyl compound (**19**) shows the best affinity with a K_i of 2.1 nM at the A_1 receptor, suggesting an optimal two to three carbon chain length of the pocket. It can also be compared favorably to the isopropyl, isobutyl, and isopentyl in terms of the width. The affinities of the compounds at the A_{2A} and A_3 adenosine receptors were only fair (the only exception being the good affinity of the cyclopropyl derivative, $K_i = 25$ nM for the A_3 receptor), thus showing an overall marked selectivity for the A_1 receptor. It is notable that the cyclopentyl group occurs more frequently as the compound in a series with the highest affinity for the A_1 receptor; namely, in the structurally different compounds of the imidazoquinolines,[9] the imidazoquinozalinamines,[40] the triazoloquinoxalines,[41] and the xanthines (DPCPX). This is, however, the first thorough examination of this particular area of the receptor site in such a manner. We have found that in agreement with Da Settimo et al.[31] the L_1 pocket is relatively small and compact. This hypothesis was disputed by the Bondavalli group[33] due to the good affinity at the bovine A_1 receptor of one of their compounds, which incorporated a rather large side chain. We can see clearly in our results that there is some affinity for a phenyl substituent at the human A_1 receptor too, i.e., that the pocket can accommodate a phenyl ring, but that this is not optimal.

It is also interesting to note the different requirements across the receptors. Although it has not been optimized in this paper, there is a distinct trend to be seen in the results at the A_{2A} and A_3 receptors. Affinity at the A_{2A} peaked with a relatively short narrow chain—the ethyl group at this pocket—and the A_3 affinity increased with the very smallest substituents, namely, the methyl and the cyclopropyl groups.

The adenosine A_{2B} receptor has in the past been somewhat neglected in terms of the testing of affinity of new ligands. This has often been due to the renowned low-affinity nature of the receptor, and the general difficulties involved in thus assessing the affinity without functional assays. As a result there are relatively few types of compounds possessing sufficient affinity at the adenosine A_{2B} receptor.[42] To substantiate our general observations that the 2,6-diphenyl-4-amidopyrimidines are good A_1 receptor ligands, a selection of the most potent or selective compounds at the A_1 receptor (**13**, **14**, **16**, **18**, **19**) were tested in A_{2B} binding assays. These results can be found in Table 1. These five ligands were chosen on the basis of their very good affinity for the A_1 receptor (**13**, **14**, **18**, **19**) or a combination of good affinity and a high selectivity over the A_{2A} and A_3 receptors (**16**). The two compounds (**14**, **19**) that displayed very potent affinity for the A_1 receptor, at approximately 2 nM, achieved only approximately 50% displacement of the radioligand on the A_{2B} receptor at concentrations of 1 μM. The compounds **13** and **18**, which showed slightly less affinity and less selectivity for the A_1 receptor above the A_{2A} and A_3 receptors, also displayed slightly more affinity at the A_{2B} receptor. Where the ligand was more selective for the A_1 receptor (**16**) over the A_{2A} and A_3 receptors, a lower affinity for the A_{2B} receptor was also noted. This highlights the good selectivity characteristics of compound **16** for human adenosine A_1 receptors.

Table 2 summarizes the results of the binding assays of the 4,6-diphenyl-2-amidopyrimidines (**22−40**). The (substituted) benzamides were again the first compounds to be prepared and tested. We found that the unsubstituted compound (**22**) showed relatively good affinity at both the A_1 and the A_{2A} receptors. Again, in consequence to the Topliss[39] system of substitution, the 4-position of the phenyl ring was varied first. This generally lowered the affinity of the pyrimidines at all the adenosine receptors. In previous publications, it has been shown that the A_3 adenosine receptor requires a 4-methoxy substitution to increase affinity.[13,43] However, in this series of benzamides the 4-chloro substituent showed the highest potency. The only 3-substituent (**27**) we made showed only fair affinity at the A_1 adenosine receptor, comparable to the unsubstituted phenyl compound.

As with the 2,6-diphenyl-4-amidopyrimidines, the alkyl substituents caused a substantial increase in

affinity when compared to the phenyl counterparts, suggesting perhaps that these molecules bind in a similar way (at the A₁ receptor), albeit with a different electronic pattern in the central heterocyclic core. At an affinity of 4 nM, compound **30** with an *n*-propyl substituent, was the most active ligand.

The A₃ receptor is favored by the smaller methyl and ethyl derivatives, improving on the affinity achieved by the (substituted) benzamide derivatives substantially. The extent of this resulted in a 2-fold selectivity for A₃ over A₁; compound **28** K_i (hA₁) = 480 nM vs K_i (hA₃) = 240 nM.

The branched alkyl derivatives (**33**−**36**) showed a remarkably high selectivity for the A₁ receptor over the A₂A and the A₃ receptors. With K_i values ranging from 9 to 30 nM for most of these derivatives, it can be said that they are very well suited as ligands for the A₁ adenosine receptor.

The cycloalkyl analogues were similarly good at the A₁ receptor, with the cyclopentyl substituent (**39**) having an affinity of 11 nM and good selectivity over the other two receptors. As the size of the cycloalkyl group decreased to a three-membered ring, the affinity for the other receptors increased.

Again, a few compounds were selected for assessment at the adenosine A₂B receptor on the basis of their performance at the A₁ receptor. These results are displayed in Table 2. The compounds which possessed less than or approximately 10 nM affinity at the adenosine A₁ receptor were chosen (**30**, **33**, **39**) and subjected to radioligand binding assays. The most potent and selective compound for the A₁ adenosine receptor (**30**) displayed a displacement of the radioligand in the region of only 50%, at a concentration of 1 μM. Compound **33**, which had already displayed slightly more affinity for the A₂A and A₃ receptors (at approximately 45% displacement of the radioligand at 1 μM concentrations) than compound **30** also displayed slightly stronger affinity for the A₂B receptor at 79% displacement of the radioligand at 1 μM concentration. Displacement of the radioligand at the A₂B receptor by compound **39** at 1 μM was less than 50%. In general, on the basis of the results shown in Tables 1 and 2, compounds with a high selectivity for the A₁ receptor over the A₂A and A₃ adenosine receptors retained that degree of selectivity over the adenosine A₂B receptor.

If we assume that this set of ligands binds to the A₁ receptor in the same manner as the 2,6-diphenyl-4-amidopyrimidines on the basis of the comparably good affinities, there is one major difference between the two series of compounds that must therefore account for the enhanced selectivity. This is the position of the nitrogens in the ring with respect to the amide bond. The positioning of both nitrogen atoms adjacent to the amide functionality now highlights the issue of electronic interaction between the pyrimidine ring and the amide group. The close proximity of the two systems may lead to a forced conformation of the amide substituent, twisting the carbonyl group out of plane with the ring. This of course assumes that the molecule sits in the normally more energetically favorable amido form.

It is also possible that there is a shift in electrons/protons forcing a preferred iminol tautomer (see Figure 7), leaving the substituent still in the plane of the ring.
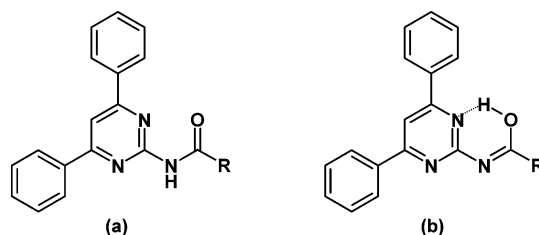

Figure 7. Two possible tautomers of the amide bond: (a) the amide form; (b) the iminol form.

This tautomerism may also be relevant to the initial series (the 4-amido-2,6-diphenylpyrimidines), but due to the close proximity of not only one, but two nitrogens (from the pyrimidine ring) to the amide group, we believe that it is of much more importance to the latter series. This type of tautomerism question has been dealt with in a previous publication in our group involving a set of isoquinolines.[38] In these compounds, it was suggested that a phenyl substituent on the amide in the same plane as that of the isoquinoline might contribute to conjugation, promoting the iminol form. In the ¹H NMR (CDCl₃) spectra where a signal was seen in the 16 ppm region it was attributed to the iminol form and where a peak was present in the 10 ppm region to the amide form. This was further corroborated with IR spectral evidence using the presence or the absence of the characteristic carbonyl shift in the 1600−1700 cm⁻¹ region. The IR spectra of the solid compounds showed that the compounds were primarily in the amide form. The similarities of the isoquinolines to the pyrimidines with respect to the positioning of the amide group adjacent to the nitrogen of the heterocycle led us also to examine the spectroscopic data of one representative compound in more detail. Compound **33** was chosen as the representative ligand due to its high affinity and good selectivity for the A₁ adenosine receptor. Although the phenyl-substituted compounds (**22**−**27**) are more similar to the isoquinoline derivatives, these were not examined in further detail due to their relatively poor affinities. The ¹H NMR (CDCl₃) of compound **33** showed clearly a signal in the 8 ppm region which corresponds to the N−H of the traditional amido form of the molecule. The use of the more polar DMSO as a NMR solvent gave a comparable spectrum. The ligand was further examined with IR spectroscopy, where a sharp carbonyl signal was present at 1680 cm⁻¹ in the solid phase, shifting to a broader signal at 1683 cm⁻¹ in chloroform. Examining compound **33** in silico, the molecules were drawn in Spartan and minimized and conformers were then generated using the systematic search method. To determine a representative and comparable energy of each tautomer, the lowest energy conformer was subjected to ab initio calculations using 3-21G* as the basis set. The resulting ΔG between the lowest energy conformers of the two tautomeric forms was 17 kcal·mol⁻¹ in favor of the amide. We therefore propose that the alkyl-substituted 2-amidopyrimidines reside in the amide tautomeric form. It should be noted, though, that the receptor-bound conformation could still be different despite the unambiguous experimental and computational evidence for the amide tautomer.

The compounds designed, synthesized, and tested in this paper show PSA values within the proposed limits for BBB penetration by Kelder.[25] To relate our com-
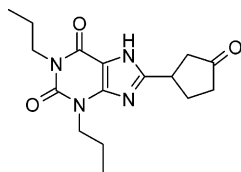
Figure 8. KFM 19.
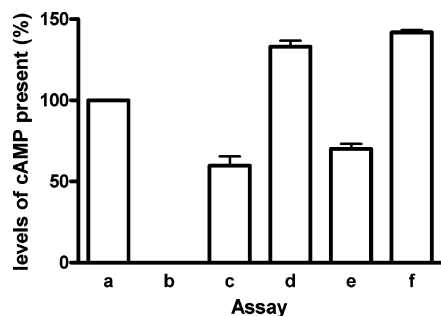
Figure 9. Functional assays for compounds **14** and **19** on the adenosine A_1 receptor: (a) levels of cAMP produced after stimulation with forskolin (10 μM); (b) the levels of cAMP detected after inhibition by the agonist CPA (1 μM); (c) cAMP levels present when forskolin (10 μM), CPA (1 μM), and compound **14** (1 μM) were introduced to the assay; (d) cAMP levels present when forskolin (10 μM), CPA (1 μM), and compound **14** (10 μM) were introduced to the assay; (e) levels of cAMP available in the presence of forskolin (10 μM), CPA (1 μM), and compound **19** (1 μM); (f) levels of cAMP available in the presence of forskolin (10 μM), CPA (1 μM), and compound **19** (10 μM). 100% cAMP amounts to approximately 15 pmol per well. 0% corresponds to approximately 1.3 pmol per well.

pounds to examples of adenosine A_1 antagonists that already display CNS activity, we calculated the PSA of two well documented molecules. The first example was caffeine (Figure 1), an adenosine antagonist with well-known CNS effects, and it was calculated by our methods to have a PSA value of 59 Å^2. Another xanthine, which was published with thorough in vivo data, is KFM 19 (the more active $S(-)$ enantiomer is known as ampaxifylline) (Figure 8).[44] This compound was administered orally to a number of different species and found to demonstrate good bioavailability. Moreover, its pharmacological profile suggested a high therapeutic potential for dementia and other cognitive deficits. We calculated the PSA value of KFM 19 to be 90 Å^2. Since the PSA values for the ligands detailed in this paper lie within or under these two values, we believe that this is further evidence to suggest that they possess the potential to be active at the CNS.

In light of recent developments in adenosine receptor research,[18,19] we performed functional assays to determine the effect of the pyrimidines at the adenosine A_1 receptor. The two best compounds (**14**, **19**) in terms of affinity at the A_1 receptor were selected (K_i = 2 nM for both compounds) and tested in cAMP assays in the presence of forskolin and N^6-cyclopentyladenosine (CPA) to assess their ability to antagonize the A_1 receptor. Figure 9 depicts the results of these experiments. Due to the adenosine A_1 receptor's coupling to an inhibitory G protein, which leads to a decrease in the levels of cAMP upon stimulation, forskolin was added to generate a measurable amount of cAMP in the system. The amount of cAMP generated by the sole addition of forskolin was thus set at 100% (Figure 9a). CPA, a well-

known full agonist of the A_1 receptor, reduced the levels of cAMP (0% for the calculations, Figure 9b). At a concentration of 1 μM, compounds **14** and **19** both displayed antagonistic behavior in the test system (Figure 9c,e). In this experimental setup the amount of cAMP measured in the system was some 60−70% of the forskolin-induced levels (Figure 9a). At higher concentrations of the compounds (10 μM), both **14** and **19** reversed the effects of CPA completely (Figure 9d and Figure 9f, respectively) to such an extent that inverse agonistic behavior was recorded. Thus the pyrimidines presented in this paper display antagonistic−inverse agonistic behavior, typical of most nonribose compounds.

Conclusion

Presented in this paper are two novel series of adenosine receptor antagonists, 2,6-diphenyl-4-amidopyrimidines and 4,6-diphenyl-2-amidopyrimidines, which have been designed and synthesized on the basis of a pharmacophore derived from the modeling of a number of previously published ligands. The idea of a monocyclic heteroaromatic core as the basis of an antagonist has been proven to be compatible with the adenosine receptor site, and one of the proposed lipophilic pockets of the site has been thoroughly investigated in terms of spatial requirements. The ligands have good affinity at the adenosine A_1 receptor, and the second set has particularly excellent selectivity over the A_{2A} and A_3 adenosine receptors. Moreover, they have a PSA of less than or approximately 60 Å^2 and, as such, meet our first simple cutoff for BBB penetration. In particular compound **30** (LUF 5735) combined high affinity (K_i = 4 nM) with high selectivity for the A_1 adenosine receptor and a PSA value of only 53 Å^2.

Experimental Section

Molecular Modeling. Molecular modeling work was performed with the SPARTAN molecular modeling package version 5.0 (Wavefunction Inc.)[30] running on a Silicon Graphics O_2 workstation. Default values in the Merck Force Field were used in Molecular Mechanics minimizations. Conjugate gradient energy minimizations were continued until the rms energy derivative was less than 0.001 kcal·mol^{-1}Å^{-1}. The conformers were generated using the systematic search method. The energy and molecular electrostatic potential was calculated using the semiempirical molecular orbital program AM1. The electrostatic potentials were sampled over the entire accessible surface of the molecules (equal to a van der Waals contact surface). The most negative electrostatic potential is red, and the most positive is blue.

The polar surface areas of the molecules were then calculated by applying Polsurf 1.0 to convert the raw data from the Spartan "input" and "proparc" files into the polar surface area of the molecule. [A copy of PolSurf and its (C) source code can be obtained from the author.] Further energy calculations on compound **33** were performed by taking the lowest energy conformer (as generated by the procedure described above) and subjecting this to ab initio calculations using 3-21G* as the basis set.

Chemistry. Materials and Methods. All reagents used were obtained from commercial sources, and all solvents were of an analytical grade. ^{1}H and ^{13}C NMR spectra were recorded on a Bruker AC 200 (^{1}H NMR, 200 MHz; ^{13}C NMR, 50.29 MHz) spectrometer with tetramethylsilane as an internal standard. Chemical shifts are reported in δ (ppm), and the following abbreviations are used: s = singlet, d = doublet, dd = double doublet, t = triplet, m = multiplet, br = broad, and ar = aromatic protons. Melting points were determined on a Büchi melting point apparatus and are uncorrected. Elemental

analyses were performed by the Leiden Institute of Chemistry and are within 0.4% of the theoretical values unless otherwise stated. Reactions were routinely monitored by TLC using Merck silica gel F$_{254}$ plates. Solid phase infrared spectra were measured with a Perkin-Elmer FT-IR Paragon 1000 spectrometer equipped with a Golden Gate Diamond ATR, using the reflectance technique (neat, 4000–300 cm^{-1}, resolution 4 cm^{-1}). Solution phase infrared spectra were recorded on a Bruker 330V IR spectrophotometer equipped with a circle liquid analyzer from Spectra Tech. (4000–300 cm^{-1}, resolution 4 cm^{-1}).

2,6-Diphenyl-3H-pyrimidin-4-one (1). Benzamidine hydrochloride (3.0 g, 19.2 mmol) was dissolved in a minimal amount of H$_2$O (10 mL). To this was added NaOH (0.8 g, 19.2 mmol, 1 equiv) dissolved in H$_2$O (2 mL), followed by ethylbenzoate (3.5 mL, 20.2 mmol, 1.05 equiv). Ethanol was then added until a clear solution was obtained. The reaction mixture was then stirred at room temperature overnight, yielding a thick suspension, which was then filtered to give a white solid. After washing with diethyl ether to remove unreacted/excess β-ketoester, the solid was dried in vacuo to give 59% of the desired product. ^{1}H NMR δ (DMSO-d_6): 8.31–8.18 (m, 5H, phenyl-*H*), 7.60–7.54 (m, 5H, phenyl-*H*), 6.92 (s, 1H, pyrimidine-*H*).

4-Chloro-2,6-diphenylpyrimidine (2). Phosphorous oxychloride (9.30 mL, 99.8 mmol, 7.5 equiv) was added dropwise to 2,6-diphenyl-3H-pyrimidin-4-one (1) (3.3 g, 13.3 mmol) in a vigorous reaction. To this mixture was added cautiously and portionwise phosphorous pentachloride (2.77 g, 13.3 mmol, 1 equiv), and the reaction mixture was stirred at reflux for 3 h. The reaction mixture was then quenched by pouring into ice–water and extracted with ethyl acetate (3 × 150 mL). The combined organic layers were washed with water and brine, dried (MgSO$_4$), and then concentrated to give a yellow solid. This was recrystallized from ethanol to give fine white needles (65%). ^{1}H NMR δ (CDCl$_3$): 8.60–8.18 (m, 5H, phenyl-*H*), 7.63 (s, 1H, pyrimidine-*H*), 7.51–7.57 (m, 5H, phenyl-*H*).

2,6-Diphenylpyrimin-4-ylamine (3). Ethanol (50 mL) was saturated with NH$_{3(g)}$ at 0 °C and added to 4-chloro-2,6-diphenylpyrimidine (2) (2.30 g, 8.63 mmol) in a sealed vessel. This was then stirred at 140 °C for 24 h. Upon cooling and concentrating, the residue was extracted with hot chloroform (3 × 50 mL) and the solvent evaporated in vacuo. The crude product was purified by column chromatography on SiO$_2$ eluting with CH$_2$Cl$_2$ to give an off-white solid (80%). ^{1}H NMR δ (DMSO-d_6): 8.47–8.42 (m, 2H, phenyl-*H*), 8.16–8.13 (m, 2H, phenyl-*H*), 7.57–7.5 (m, 6H, phenyl-*H*), 7.02 (br s, 2H, N*H*$_2$), 6.88 (s, 1H, pyrimidine-*H*).

General Procedure for the Preparation of 4-Amido-2,6-diphenylpyrimidines (4–20, 22–40). To a solution of the amino-diphenylpyrimidine (0.202 mmol, 1 equiv) in 1,4-dioxane (5 mL) was added triethylamine (0.223 mmol, 1.1 equiv), followed by the appropriate acid chloride (0.304 mmol, 1.5 equiv). This was then stirred at reflux until no starting material was visible by TLC. Upon completion, the reaction mixture was separated between ethyl acetate (20 mL) and water (20 mL). The aqueous layer was further extracted with ethyl acetate (2 × 20 mL), and the combined organics were washed with water and brine. After drying over MgSO$_4$ and evaporation under reduced pressure, the crude product was purified by column chromatography, eluting with a petroleum ether–ethyl acetate or a dichloromethane–methanol solvent system. Recrystallization from ethanol or petroleum ether–ethyl acetate gave the corresponding amide in crystalline form.

N-(2,6-Diphenylpyrimidin-4-yl)benzamide (4). Yield: 48%; white solid. ^{1}H NMR δ (CDCl$_3$): 8.78 (br s, 1H, N-*H*), 8.72 (s, 1H, pyrimidine-*H*), 8.58–8.54 (m, 2H, phenyl-*H*), 8.34–8.29 (m, 2H, phenyl-*H*), 7.99–7.96 (m, 2H, phenyl-*H*), 7.64–7.48 (m, 9H, phenyl-*H*). Anal. (C$_{23}$H$_{17}$N$_3$O·0.3H$_2$O) C, H, N.

4-Chloro-N-(2,6-diphenylpyrimidin-4-yl)benzamide (5). Yield: 57%; white solid. ^{1}H NMR δ (CDCl$_3$): 8.70 (br s, 1H, N-*H*), 8.68 (s, 1H, pyrimidine-*H*), 8.57–8.52 (m, 2H, phenyl-*H*), 8.33–8.28 (m, 2H, phenyl-*H*), 7.93–7.89 (m, 2H, aromatic-*H*), 7.56–7.49 (m, 8H, phenyl-*H*). Anal. (C$_{23}$H$_{16}$ClN$_3$O) C, H, N.

N-(2,6-Diphenylpyrimidin-4-yl)-4-methoxybenzamide) (6). Yield: 12%; white solid. ^{1}H NMR δ (CDCl$_3$): 8.73 (s, 1H, pyrimidine-*H*), 8.67 (br s, 1H, N-*H*), 8.59–8.54 (m, 2H, phenyl-*H*), 8.34–8.29 (m, 2H, phenyl-*H*), 8.00–7.96 (m, 2H, aromatic-*H*), 7.55–7.51 (m, 6H, phenyl-*H*), 7.06–7.02 (m, 2H, aromatic-*H*), 3.91 (s, 3H, C*H*$_3$). Anal. (C$_{24}$H$_{19}$N$_3$O$_2$·0.4H$_2$O) C, H, N.

N-(2,6-Diphenylpyrimidin-4-yl)acetamide (7). Yield: 43%; white solid. ^{1}H NMR δ (CDCl$_3$): 8.54–8.49 (m, 3H, phenyl-*H* + pyrimidine-*H*), 8.45 (s, 1H, N-*H*), 7.55–7.49 (m, 6H, phenyl-*H*), 2.20 (s, 3H, C*H*$_3$). Anal. (C$_{18}$H$_{15}$N$_3$O·0.5EtOH) C, H, N.

N-(2,6-Diphenylpyrimidin-4-yl)propionamide (8). Yield: 77%; white solid. ^{1}H NMR δ (CDCl$_3$): 8.58 (s, 1H, pyrimidine-*H*), 8.55–8.50 (m, 2H, phenyl-*H*), 8.36 (br s, 1H, N*H*), 8.30–8.25 (m, 2H, phenyl-*H*), 7.54–7.49 (m, 6H, phenyl-*H*), 2.41 (q, 2H, *J* = 7.3 Hz, C*H*$_2$CH$_3$), 1.23 (t, 2H, –CH$_2$C*H*$_3$). Anal. Calcd for C$_{19}$H$_{17}$N$_3$O (C 75.23; H 5.65; N 13.85), found (C 75.32; H 6.23; N 14.04).

N-(2,6-Diphenylpyrimidin-4-yl)butyramide (9). Yield: 45%; white solid. ^{1}H NMR δ (CDCl$_3$): 8.60 (br s, 2H, pyrimidine-*H* + N*H*), 8.56–8.51 (m, 2H, phenyl-*H*), 8.31–8.26 (m, 2H, phenyl-*H*), 7.45–7.50 (m, 6H, phenyl-*H*), 2.29 (t, 2H, *J* = 7.48 Hz, C*H*$_2$CH$_2$CH$_3$), 1.71 (sextet, 2H, *J* = 7.39 Hz, CH$_2$C*H*$_2$-CH$_3$), 0.95 (t, 3H, *J* = 7.30 Hz, CH$_2$CH$_2$C*H*$_3$). Anal. (C$_{20}$H$_{19}$N$_3$O·0.1H$_2$O) C, H, N.

Hexanoic Acid (2,6-Diphenylpyrimidin-4-yl)amide (10). Yield: 53%; white solid. ^{1}H NMR δ (CDCl$_3$): 8.53 (s, 1H, pyrimidine-*H*), 8.52–8.49 (m, 2H, phenyl-*H*,) 8.30–8.23 (m, 3H, phenyl-*H* + N-*H*), 7.55–7.47 (m, 6H, phenyl-*H*), 2.43 (t, 2H, *J* = 7.30 Hz, C*H*$_2$CH$_2$CH$_2$CH$_2$CH$_3$), 1.82–1.67 (m, 2H, CH$_2$C*H*$_2$CH$_2$CH$_2$CH$_3$), 1.41–1.21 (m, 4H, CH$_2$CH$_2$C*H*$_2$C*H*$_2$-CH$_3$), 0.96–1.89 (m, 3H, CH$_2$CH$_2$CH$_2$CH$_2$C*H*$_3$). Anal. (C$_{22}$H$_{23}$-N$_3$O·1.7H$_2$O) C, H, N.

N-(2,6-Diphenylpyrimidin-4-yl)isobutyramide (11). Yield: 39%; white solid. ^{1}H NMR δ (CDCl$_3$): 8.59 (s, 1H, pyrimidine-*H*), 8.55–8.50 (m, 2H, phenyl-*H*), 8.30–8.25 (m, 2H, phenyl-*H*), 8.05 (br s, 1H, N*H*), 7.54–7.49 (m, 6H, phenyl-*H*), 2.64 (septet, 1H, *J* = 6.85 Hz, C*H*(CH$_3$)$_2$), 1.33 (d, 6H, *J* = 6.94 Hz, CH(C*H*$_3$)$_2$). Anal. (C$_{20}$H$_{19}$N$_3$O·0.1H$_2$O) C, H, N.

N-(2,6-Diphenylpyrimidin-4-yl)-3-methylbutyramide (12). Yield: 52%; white solid. ^{1}H NMR δ (CDCl$_3$): 8.59 (s, 1H, pyrimidine-*H*), 8.56–8.51 (m, 2H, phenyl-*H*), 8.35 (br s, 1H, N*H*), 8.31–8.26 (m, 2H, phenyl-*H*), 7.56–7.49 (m, 6H, phenyl-*H*), 2.25–2.24 (m, 3H, C*H*$_2$C*H*(CH$_3$)$_2$), 1.02–0.99 (d, 6H, CH$_2$-CH(C*H*$_3$)$_2$). Anal. (C$_{21}$H$_{21}$N$_3$O) C, H, N.

N-(2,6-Diphenylpyrimidin-4-yl)-2-ethylbutyramide (13). Yield: 66%; white solid. ^{1}H NMR δ (CDCl$_3$): 8.64 (s, 1H, pyrimidine-*H*), 8.55–8.50 (m, 2H, phenyl-*H*), 8.31–8.26 (m, 2H, phenyl-*H*), 8.09 (br s, 1H, N*H*), 7.54–7.49 (m, 6H, phenyl-*H*), 2.23–2.11 (m, 1H, C*H*(CH$_2$CH$_3$)$_2$), 1.86–1.56 (m, 4H, CH-(C*H*$_2$CH$_3$)$_2$), 0.99 (t, 6H, *J* = 7.31 Hz, CH(CH$_2$C*H*$_3$)$_2$). Anal. (C$_{22}$H$_{23}$N$_3$O·0.1H$_2$O) C, H, N.

N-(2,6-Diphenylpyrimidin-4-yl)-2-methylbutyramide (14). Yield: 89%; white solid. ^{1}H NMR δ (CDCl$_3$): 8.71 (br s, 1H, N-*H*), 8.67 (s, 1H, pyrimidine-*H*), 8.59–8.54 (m, 2H, aromatic-*H*), 8.33–8.28 (m, 2H, aromatic-*H*), 7.53–7.50 (m, 6H, aromatic-*H*), 2.29–2.19 (m, 1H, CH), 1.82–1.86 (m, 1H, 0.5*C*H*$_2$), 1.55–1.41 (m, 1H, 0.5*C*H*$_2$), 1.16 (d, *J* = 6.58 Hz, 3H, C*H*$_3$), 0.90 (t, *J* = 7.30 Hz, 3H, C*H*$_3$). Anal. (C$_{21}$H$_{21}$N$_3$O) C, H, N.

N-(2,6-Diphenylpyrimidin-4-yl)-2,2-dimethylpropionamide (15). Yield: 66%; white solid. ^{1}H NMR δ (CDCl$_3$): 8.63 (s, 1H, pyrimidine-*H*), 8.58–8.51 (m, 2H, phenyl-*H*), 8.30–8.27 (m, 2H, phenyl-*H*), 8.21 (s, 1H, N-*H*), 7.54–7.51 (m, 6H, phenyl-*H*), 1.40 (s, 9H, C*H*$_3$). Anal. (C$_{21}$H$_{21}$N$_3$O) C, H, N.

N-(2,6-Diphenylpyrimidin-4-yl)-3,3-dimethylbutyramide (16). Yield: 62%; white solid. ^{1}H NMR δ (CDCl$_3$): 8.73 (br s, 1H, N-*H*), 8.64 (s, 1H, pyrimidine-*H*), 8.55–8.50 (m, 2H, aromatic-*H*), 8.32–8.27 (m, 2H, aromatic-*H*), 7.54–7.49 (m, 11H, aromatic-*H*), 2.20 (s, 2H, CH$_2$), 1.08 (s, 9H, 3*C*H*$_3$). Anal. (C$_{22}$H$_{23}$N$_3$O) C, H, N.

Cyclopropanecarboxylic Acid (2,6-Diphenylpyrimidin-4-yl)amide (17). Yield: 86%; white solid. ^{1}H NMR δ (CDCl$_3$): 8.99 (br s, 1H, N*H*), 8.58 (s, 1H, pyrimidine-*H*), 8.56–

8.52 (m, 2H, phenyl-*H*), 8.29–8.24 (m, 2H, phenyl-*H*), 7.53–7.49 (m, 6H, phenyl-*H*), 1.47–1.43 (m, 1H, −C*H*CH$_2$CH$_2$−), 1.11–1.05 (m, 2H, −CHC*H$_2$*CH$_2$−), 0.86–0.76 (m, 2H, −CHCH$_2$-C*H$_2$*−). Anal. (C$_{20}$H$_{17}$N$_3$O) C, H, N.

Cyclobutanecarboxylic Acid (2,6-Diphenylpyrimidin-4-yl)amide (18). Yield: 90%; white solid. ^{1}H NMR δ (CDCl$_3$): 8.62 (s, 1H, pyrimidine-*H*), 8.56–8.51 (m, 2H, phenyl-*H*), 8.32–8.27 (m, 3H, phenyl-*H* + N-*H*), 7.54–7.48 (m, 6H, phenyl-*H*), 3.13 (pentet, 1H, −C*H*CH$_2$CH$_2$CH$_2$−), 2.45–1.90 (m, 6H, −CHC*H$_2$*C*H$_2$*CH$_2$−). Anal. (C$_{21}$H$_{19}$N$_3$O·0.1H$_2$O) C, H, N.

Cyclopentanecarboxylic Acid (2,6-Diphenylpyrimidin-4-yl)amide (19). Yield: 69%; white solid. ^{1}H NMR δ (CDCl$_3$): 8.60 (s, 1H, pyrimidine-*H*), 8.56–8.51 (m, 2H, phenyl-*H*), 8.32–8.26 (m, 3H, phenyl-*H* + N*H*), 7.53–7.50 (m, 6H, phenyl-*H*), 2.77–2.65 (m, 1H, −C*H*CH$_2$CH$_2$CH$_2$CH$_2$−), 1.98–1.60 (m, 8H, −CHC*H$_2$*C*H$_2$*C*H$_2$*C*H$_2$*−). Anal. (C$_{22}$H$_{21}$N$_3$O·0.1H$_2$O) C, H, N.

Cyclohexanecarboxylic Acid (2,6-Diphenylpyrimidin-4-yl)amide (20). Yield: 87%; white solid. ^{1}H NMR δ (CDCl$_3$): 8.60 (s, 1H, pyrimidinel-*H*), 8.57–8.52 (m, 2H, phenyl-*H*), 8.34 (br s, 1H, N*H*), 8.30–8.25 (m, 2H, phenyl-*H*), 7.53–7.49 (m, 6H, phenyl-*H*), 2.31–2.18 (m, 1H, −C*H*CH$_2$CH$_2$CH$_2$CH$_2$-CH$_2$−), 1.97–1.30 (m, 10H, −CHC*H$_2$*C*H$_2$*C*H$_2$*C*H$_2$*C*H$_2$*−). Anal. (C$_{23}$H$_{23}$N$_3$O·0.2H$_2$O) C, H, N.

2-Amino-4,6-diphenylpyrimidine (21). A mixture of benzylidenacetophenone (38.6 g, 0.185 mol, 1.1 equiv) and guanidine hydrochloride (16 g, 0.168 mol, 1 equiv) was refluxed in ethanol (150 mL). Sodium hydroxide (21.6 g, 0.539 mol, 3.2 equiv) was dissolved in a minimum amount of water (40 mL) and added dropwise to the refluxing mixture. The reaction mixture was then stirred at reflux for a further 6 h. Upon cooling, the reaction mixture was concentrated and then separated between ethyl acetate (200 mL) and water (200 mL). The aqueous layer was then extracted with ethyl acetate (2 × 100 mL). The combined organic layers were washed with water (200 mL) and brine (200 mL), dried over MgSO$_4$, and concentrated in vacuo. The crude product was purified by column chromatography on SiO$_2$, eluting with dichloromethane. Recrystallization from ethyl acetate gave clear colorless crystals; yield 31%. ^{1}H NMR δ (CDCl$_3$): 8.09–8.04 (m, 4H, phenyl-*H*), 7.54–7.48 (m, 7H, phenyl-*H*), 5.25 (br s, 2H, NH$_2$).

N-(4,6-Diphenylpyrimidin-2-yl)benzamide (22). Yield: 34%; white solid. ^{1}H NMR δ (CDCl$_3$): 8.75 (br s, 1H, N-*H*), 8.22–8.17 (m, 4H, phenyl-*H*), 8.02–7.98 (m, 2H, phenyl-*H*), 7.90 (s, 1H, pyrimidine-*H*), 7.56–7.52 (m, 9H, phenyl-*H*). Anal. Calcd for (C$_{23}$H$_{17}$N$_3$O) (C 78.61; H 4.88; N 11.96), found (C 78.20; H 4.88; N 12.38).

N-(4,6-Diphenylpyrimidin-2-yl)-4-chlorobenzamide (23). Yield: 82%; white solid. ^{1}H NMR δ (CDCl$_3$): 8.86 (br s, 1H, N-*H*), 8.15–8.11 (m, 2H, phenyl-*H*), 7.88–7.85 (m, 3H, phenyl-*H*), 7.53–7.41 (m, 8H, phenyl-*H*). Anal. (C$_{23}$H$_{16}$ClN$_3$O·0.2H$_2$O) C, H, N.

N-(4,6-Diphenylpyrimidin-2-yl)-4-methoxybenzamide (24). Yield: 27%; white solid; mp 155 °C. ^{1}H NMR δ (CDCl$_3$): 8.82 (br s, 1H, N*H*), 8.22–8.13 (m, 4H, phenyl-*H*), 7.99–7.92 (d, 2H, phenyl-*H*), 7.85 (s, 1H, pyrimidinyl-*H*), 7.53–7.48 (m, 6H, phenyl-*H*), 7.00–6.93 (d, 2H, phenyl-*H*), 3.86 (s, 3H, C*H$_3$*). Anal.(C$_{24}$H$_{19}$N$_3$O$_2$·3H$_2$O) C, H, N.

N-(4,6-Diphenylpyrimidin-2-yl)-4-methylbenzamide (25). Yield: 22%; white solid. ^{1}H NMR δ (CDCl$_3$): 8.76 (br s, 1H, N*H*), 8.23–8.18 (m, 4H, phenyl-*H*), 7.94 (d, 2H, phenyl-*H*), 7.90 (s, 1H, pyrimidinyl-*H*), 7.56–7.53 (m, 6H, phenyl-*H*), 7.36–7.32 (d, 2H, phenyl-*H*), 2.46 (s, 3H, C*H$_3$*). Anal. (C$_{24}$H$_{19}$N$_3$O·0.2H$_2$O) C, H, N.

3,4-Dichloro-N-(4,6-diphenylpyrimidin-2-yl)benzamide (26). Yield: 13%; white solid. ^{1}H NMR δ (CDCl$_3$): 8.67 (br s, 1H, N*H*), 8.18–8.11 (m, 4H, phenyl-*H*), 8.08–8.07 (m, 1H, phenyl-*H*), 7.93 (s, 1H, pyrimidinyl-*H*), 7.83–7.78 (m, 1H, phenyl-*H*), 7.64–7.51 (m, 7H, phenyl-*H*). Anal. (C$_{23}$H$_{15}$Cl$_2$N$_3$O·1.3H$_2$O) C, H, N.

N-(4,6-Diphenylpyrimidin-2-yl)-3-chlorobenzamide (27). Yield: 98%; white solid. ^{1}H NMR δ (CDCl$_3$): 8.96 (br s, 1H, N*H*), 8.16–8.11 (m, 4H, phenyl-*H*), 7.91–7.89 (m, 1H, phenyl-*H*), 7.85 (s, 1H, pyrimidinyl-*H*), 7.81–7.77 (m, 1H, phenyl-

7.54–7.45 (m, 6H, phenyl-*H*), 7.42–7.35 (m, 2H, phenyl-*H*). Anal. (C$_{23}$H$_{16}$ClN$_3$O·0.2H$_2$O) C, H, N.

N-(4,5-Diphenylpyrimidin-2-yl)acetamide (28). Yield: 43%; white solid; mp 217–218 °C (lit. 226–227 °C).[45] ^{1}H NMR δ (CDCl$_3$): 8.15–8.10 (m, 5H, phenyl-*H* + N-*H*), 7.83 (s, 1H, pyrimidinyl-*H*), 7.56–7.53 (m, 6H, phenyl-*H*), 2.76 (s, 3H, C*H$_3$*). Anal.(C$_{18}$H$_{17}$N$_3$O·0.2H$_2$O) C, H, N.

N-(4,6-Diphenylpyrimidin-2-yl)propionamide (29). Yield: 21%; white solid. ^{1}H NMR δ (CDCl$_3$): 8.17–8.08 (m, 5H, phenyl-*H* + N*H*), 7.81 (s, 1H, pyrimidinyl-*H*), 7.56–7.50 (m, 6H, phenyl-*H*), 3.05 (q, 2H, J = 7.30 Hz, C*H$_2$*CH$_3$), 1.32 (t, 3H, J = 7.31 Hz, CH$_2$C*H$_3$*). Anal.(C$_{19}$H$_{17}$N$_3$O·0.2H$_2$O) C, H, N.

N-(4,6-Diphenylpyrimidin-2-yl)butyramide (30). Yield: 47%; white solid. ^{1}H NMR δ (CDCl$_3$): 8.16–8.09 (m, 4H, phenyl-*H*), 8.08 (br s, 1H, N*H*), 7.83 (s, 1H, pyrimidinyl-*H*), 7.55–7.52 (m, 6H, phenyl-*H*), 3.02 (t, 2H, J = 7.30 Hz, C*H$_2$*-CH$_2$CH$_3$), 1.86 (sextet, 2H, J = 7.30 Hz, CH$_2$C*H$_2$* CH$_3$), 1.08 (t, 3H, J = 7.30 Hz, CH$_2$CH$_2$C*H$_3$*). Anal. (C$_{20}$H$_{19}$N$_3$O) C, H, N.

Pentanoic Acid (4,6-Diphenylpyrimidin-2-yl)amide (31). Yield: 32%; white solid. ^{1}H NMR δ (CDCl$_3$): 8.16–8.11 (m, 4H, phenyl-*H*), 8.09 (br s, 1H, N*H*), 7.82 (s, 1H, pyrimidinyl-*H*), 7.56–7.52 (m, 6H, phenyl-*H*), 3.05 (t, 2H, J = 7.67 Hz, C*H$_2$*CH$_2$CH$_2$CH$_3$), 1.86–1.74 (m, 2H, CH$_2$C*H$_2$*CH$_2$CH$_3$), 1.58–1.40 (m, 2H, CH$_2$CH$_2$C*H$_2$*CH$_3$), 0.99 (t, 3H, J = 7.30 Hz, CH$_2$-CH$_2$CH$_2$C*H$_3$*). Anal. (C$_{21}$H$_{21}$N$_3$O·0.2H$_2$O) C, H, N.

Hexanoic Acid (4,6-Diphenylpyrimidin-2-yl)amide (32). Yield: 86%; white solid. ^{1}H NMR δ (CDCl$_3$): 8.30 (br s, 1H, N*H*), 8.14–8.09 (m, 4H, phenyl-*H*), 7.79 (s, 1H, pyrimidinyl-*H*), 7.54–7.50 (m, 6H, phenyl-*H*), 3.00 (t, 2H, J = 7.67 Hz, C*H$_2$*CH$_2$CH$_2$CH$_2$CH$_3$), 1.86–1.78 (m, 2H, CH$_2$C*H$_2$*CH$_2$CH$_2$-CH$_3$), 1.46–1.41 (m, 4H, CH$_2$CH$_2$C*H$_2$*C*H$_2$*CH$_3$), 0.93 (m, 3H, CH$_2$CH$_2$CH$_2$CH$_2$C*H$_3$*). Anal. (C$_{22}$H$_{23}$N$_3$O) C, H, N.

N-(4,6-Diphenylpyrimidin-2-yl)isobutyramide (33). Yield: 39%; white solid. ^{1}H NMR δ (CDCl$_3$): 8.17–8.10 (m, 4H, phenyl-*H*), 8.09 (br s, 1H, N*H*), 7.84 (s, 1H, pyrimidinyl-*H*), 7.56–7.51 (m, 6H, phenyl-*H*), 3.41–3.38 (m, 1H, C*H*(CH$_3$)$_2$), 1.35 (d, 6H, J = 6.94 Hz, CH(C*H$_3$*)$_2$). Anal. (C$_{20}$H$_{19}$N$_3$O) C, H, N.

N-(4,6-Diphenylpyrimidin-2-yl)-2,2-dimethylpropionamide (34). Yield: 64%; white solid. ^{1}H NMR δ (CDCl$_3$): 8.29 (br s, 1H, N*H*), 8.20–8.14 (m, 4H, phenyl-*H*), 7.82 (s, 1H, pyrimidinyl-*H*), 7.51–7.48 (m, 6H, phenyl-*H*), 1.39 (s, 9H, 3× C*H$_3$*). Anal. (C$_{21}$H$_{21}$N$_3$O·0.2H$_2$O) C, H, N.

N-(4,6-Diphenylpyrimidin-2-yl)-3-methylbutyramide (35). Yield: 48%; white solid. ^{1}H NMR δ (CDCl$_3$): 8.27 (br s, 1H, N*H*), 8.15–8.07 (m, 4H, phenyl-*H*), 7.79 (s, 1H, pyrimidinyl-*H*), 7.55–7.47 (m, 6H, phenyl-*H*), 2.87 (d, 2H, J = 7.30, C*H$_2$*), 2.40–2.26 (m, 1H, C*H*), 1.06 (d, 6H, J = 6.94, 2× C*H$_3$*). Anal. (C$_{21}$H$_{21}$N$_3$O·0.3H$_2$O) C, H, N.

N-(4,6-Diphenylpyrimidin-2-yl)-2-ethylbutyramide (36). Yield: 22%; white solid. ^{1}H NMR δ (CDCl$_3$): 8.18–8.13 (m, 4H, phenyl-*H*), 8.11 (br s, 1H, N*H*), 7.84 (s, 1H, pyrimidinyl-*H*), 7.56–7.51 (m, 6H, phenyl-*H*), 2.97 (m, 1H, C*H*(CH$_2$CH$_3$)$_2$), 1.94–1.59 (m, 4H, CH(C*H$_2$*CH$_3$)$_2$), 1.02 (t, 6H, J = 7.30 Hz, CH(CH$_2$C*H$_3$*)$_2$). Anal. (C$_{22}$H$_{23}$N$_3$O) C, H, N.

Cyclopropane Carboxylic Acid (4,6-Diphenylpyrimidin-2-yl)amide (37). Yield: 57%; white solid. ^{1}H NMR δ (CDCl$_3$): 8.77 (br s, 1H, N*H*), 8.13–8.08 (m, 4H, phenyl-*H*), 7.78 (s, 1H, pyrimidinyl-*H*), 7.51–7.47 (m, 6H, phenyl-*H*), 2.67 (m, 1H, −C*H*CH$_2$CH$_2$−), 1.29–1.21 (m, 2H, CHC*H$_2$*CH$_2$−), 0.99–0.90 (m, 2H, −CHCH$_2$C*H$_2$*−). Anal. (C$_{20}$H$_{17}$N$_3$O) C, H, N.

Cyclobutane Carboxylic Acid (4,6-Diphenylpyrimidin-2-yl)amide (38). Yield: 98%; white solid. ^{1}H NMR δ (CDCl$_3$): 8.35 (br s, 1H, N*H*), 8.13–8.08 (m, 4H, phenyl-*H*), 7.76 (s, 1H, pyrimidinyl-*H*), 7.52–7.48 (m, 6H, phenyl-*H*), 4.05–3.96 (m, 1H, −C*H*CH$_2$CH$_2$CH$_2$−), 2.57–2.21 (m, 4H, −CHC*H$_2$*CH$_2$-C*H$_2$*−), 2.09–1.92 (m, 2H, −CHCH$_2$C*H$_2$*CH$_2$−). Anal. (C$_{21}$H$_{19}$N$_3$O·0.1H$_2$O) C, H, N.

Cyclopentane Carboxylic Acid (4,6-Diphenylpyrimidin-2-yl)amide (39). Yield: 98%; white solid. ^{1}H NMR δ (CDCl$_3$): 8.16–8.11 (m, 4H, phenyl-*H*), 7.82 (s, 1H, pyrimidi-

nyl-*H*), 7.55−7.51 (m, 6H, phenyl-*H*), 2.04−1.65 (m, 9H, cyclopentane). Anal. ($C_{22}H_{21}N_3O\cdot0.1H_2O$) C, H, N.

Cyclohexanecarboxylic Acid (4,6-Diphenylpyrimidin-2-yl)amide (40). Yield: 26%; white solid. ^1H NMR δ (CDCl3): 8.11−8.19 (m, 4H, phenyl-*H*), 7.83 (s, 1H, pyrimidinyl-*H*), 7.50−7.57 (m, 6H, phenyl-*H*), 0.83−2.10 (m, 11H, C*H*$_2$ + C*H*). Anal. ($C_{23}H_{23}N_3O\cdot0.2H_2O$) C, H, N.

Biology. Materials and Methods. [³H]DPCPX and [¹²⁵I]-AB-MECA were purchased from Amersham Biosciences (NL). [³H]ZM241385 and [³H]MRS1754 were obtained from Tocris Cookson, Ltd. (UK). CHO cells expressing the human adenosine A₁ receptor were provided by Dr. Andrea Townsend-Nicholson, University College of London, UK. HEK 293 cells stably expressing the human adenosine A₂ₐ and A₃ receptor were gifts from Dr. Wang (Biogen) and Dr. K.-N. Klotz (University of Würzburg, Germany), respectively. CHO cells expressing the human A₂ᵦ receptor were provided by Dr. Steve Rees (GlaxoSmithKline, UK).

All compounds made were tested in radioligand binding assays to determine their affinities at the human adenosine A₁, A₂ₐ, and the A₃ receptors, whereas a selection of the compounds were tested at the human A₂ᵦ receptor (see text).

Adenosine A₁ Receptor. Affinity at the A₁ receptor was determined on membranes from CHO cells expressing the human receptors, using [³H]DPCPX as the radioligand. Membranes containing 40 μg of protein were incubated in a total volume of 400 μL of 50 mM Tris/HCl (pH 7.4) and [³H]DPCPX (final concentration 1.6 nM) for 1 h at 25 °C in a shaking water bath. Nonspecific binding was determined in the presence of 10 μM CPA. The incubation was terminated by filtration over Whatman GF/B filters under reduced pressure with a Brandell harvester. Filters were washed three times with ice-cold buffer and placed in scintillation vials. Emulsifier Safe (3.5 mL) was added, and after 2 h radioactivity was counted in an LKB rack β scintillation counter.

Adenosine A₂ₐ Receptor. At the A₂ₐ receptor, affinity was determined on membranes from HEK 293 cells stably expressing this receptor, using [³H]ZM241385 as the radioligand. Membranes containing 40 μg of protein were incubated in a total volume of 400 μL of 50 mM Tris/HCl (pH 7.4) and [³H]-ZM241385 (final concentration 2.0 nM) for 2 h at 25 °C in a shaking water bath. Nonspecific binding was determined in the presence of 100 μM CPA. The incubation was terminated by filtration over Whatman GF/B filters under reduced pressure with a Brandell harvester. Filters were washed three times with ice-cold buffer and placed in scintillation vials. Emulsifier Safe (3.5 mL) was added, and after 2 h radioactivity was counted in an LKB rack β scintillation counter.

Adenosine A₂ᵦ Receptor. At the A₂ᵦ receptor, radioligand displacement was determined on membranes from CHO cells stably transfected with human A₂ᵦ receptor, using [³H]-MRS1754 as the radioligand. Membranes containing 20 μg of protein were incubated in a total volume of 100 μL of 50 mM Tris/HCl (pH 7.4), 10 mM MgCl₂, 1 mM EDTA, 0.01 w/v % CHAPS (pH 8.26 at 5 °C), and [³H]MRS1754 (final concentration 1.2 nM) for 1 h at 25 °C in a shaking water bath. Nonspecific binding was determined in the presence of 1 mM NECA. The incubation was terminated by filtration over Whatman GF/B filters under reduced pressure with a Brandell harvester. Filters were washed three times with ice-cold buffer and placed in scintillation vials. Emulsifier Safe (3.5 mL) was added, and after 2 h radioactivity was counted in an LKB rack β scintillation counter.

Adenosine A₃ Receptor. The affinity at the A₃ receptor was measured on membranes from HEK 293 cells stably expressing the human A₃ receptor, using [¹²⁵I]AB-MECA as the radioligand. Membranes containing 20−40 μg of protein were incubated in a total volume of 100 μL of 50 mM Tris/HCl, 10 mM MgCl₂, 1 mM EDTA, 0.01% CHAPS (pH 7.4), and [¹²⁵I]AB-MECA (final concentration 0.10 nM) for 1 h at 37 °C in a shaking water bath. Nonspecific binding was determined in the presence of 100 μM R-PIA. The incubation was terminated by filtration over Whatman GF/B filters under reduced pressure with a Brandell harvester. Filters were washed three

times with ice-cold buffer and placed in scintillation vials. Radioactivity was counted in a γ counter.

Functional Assays. CHO cells expressing the human adenosine A₁ receptor were grown overnight as a monolayer in 24 well tissue culture plates (400 μL/well; 2 × 10⁵ cells/well). cAMP generation was performed in Dulbecco's modified Eagle's medium (DMEM/ *N*-2-hydroxyethylpiperazine-*N*′-2-ethansulfonic acid (HEPES) buffer (0.60 g HEPES/50 mL DMEM pH 7.4). Each well was washed twice with HEPES/DMEM buffer (250 μL), and the following added: adenosine deaminase (0.8 IU/mL), rolipram (50 μM), cilostamide (50 μM). This was then incubated for 30 min at 37 °C followed by the introduction of CPA (1 μM) and then the compound of interest (1 μM). After a further 10 min of incubation, forskolin was added (10 μM). After a subsequent 15 min, incubation was stopped by aspirating the assay medium and by adding 200 μL of ice-cold 0.1 M HCl. The amount of cAMP was determined by competition with [³H]cAMP for protein kinase A (PKA). Briefly, the sample, approximately 1.8 nM [³H]cAMP, and 100 μL of PKA solution were incubated on ice for 2.5 h. The incubations were stopped by rapid dilution with 2 mL of ice-cold Tris HCl buffer (pH 7.4), and bound radioactive material was then recovered by filtration through Whatman GF/C filters. Filters were additionally rinsed with 2 × 2 mL of Tris HCl buffer, and then the radioactivity was counted in Packard Emulsifier Safe scintillation fluid (3.5 mL). All data reflect three independent experiments performed in duplicate.

Data Analysis. K_i values were calculated using a nonlinear regression curve-fitting program (GraphPad Prism, GraphPad Software Inc., San Diego, CA). K_D values of the radioligands were 1.6 nM, 1.0 nM, 1.3 nM, and 5.0 nM for [³H]DPCPX, [³H]-ZM241385, [³H]MRS1754, and [¹²⁵I]AB-MECA, respectively. The data from the functional assays were also analyzed with GraphPad Prism. Figure 9 was generated by evaluating the data to relate to full agonism by the known ligand CPA and the generation of cAMP by forskolin. The calculations involved the normalization of the raw data with respect to CPA (percentage of cAMP in this system set at 0) and forskolin (percentage of cAMP present in this system set at 100).

Supporting Information Available: The data showing the Polsurf calculated PSA values compared to the Clark PSA values[10,11] and a plot of the linear correlation and calculated R^2, further spectroscopic data (¹³C and MS) and melting point values for compounds **4**−**20** and **22**−**40**, and a table of the elemental analyses. This material is available free of charge via the Internet at http://pubs.acs.org.

References

(1) Fredholm, B. B.; IJzerman, A. P.; Jacobson, K. A.; Klotz, K.-N.; Linden, J. M. International Union of Pharmacology. XXV. Nomenclature and Classification of Adenosine Receptors. *Pharmacol. Rev.* **2001**, *53*, 527−552.

(2) van Galen, P. J. M.; Vlijmen, H. W. Th.; IJzerman, A. P.; Soudijn, W. A Model for the Antagonist Binding Site on the Adenosine A₁ Receptor, Based on Steric, Electrostatic, and Hydrophobic Properties. *J. Med. Chem.* **1990**, *33*, 1708−1713.

(3) Peet, N. P.; Lentz, N. L.; Meng, E. C.; Dudley, M. W.; Ogden, A. M. L.; Demeter, D. A.; Weintraub, H. J. R.; Bey, P. A Novel Synthesis of Xanthines: Support for a New Binding Mode for Xanthines with Respect to Adenosine at Adenosine Receptors. *J. Med. Chem.* **1990**, *33*, 3127−3130.

(4) Dooley, M. J.; Quinn, R. J. The Three Binding Domain Model of Adenosine Receptors: Molecular Modeling Aspects. *J. Med. Chem.* **1992**, *35*, 211−216.

(5) Dooley, M. J.; Kono, M.; Suzuki, F. Theoretical Structure-Activity Studies of Adenosine A₁ Ligands: Requirements for Receptor Affinity. *Bioorg. Med. Chem.* **1996**, *4*, 923−934.

(6) Ferrarini, R. L.; Mori, C.; Manera, C.; Martinelli, A.; Mori, F.; Saccomanni, G.; Barili, P. L.; Betti, L.; Giannaccini, G.; Trincavelli, L.; Lucacchini, A. A Novel Class of Highly Potent and Selective A₁ Adenosine Antagonists: Structure−Affinity Profile of a Series of 1,8-Naphthyridine Derivatives. *J. Med. Chem.* **2000**, *43*, 2814−2823.

(7) Hess, S.; Muller, C. E.; Frobenius, W.; Reith, U.; Klotz, K.-N.; Eger, K. 7-Deazaadenines Bearing Polar Substituents: Structure−Activity Relationships of New A$_1$ and A$_3$ Adenosine Receptor Antagonists. *J. Med. Chem.* **2000**, *43*, 4636−4646.

(8) Chebib, M.; McKeveney, D., Quinn, R. J. 1-Phenylpyrazolo[3,4-*d*]pyrimidines; Structure-Acitivity Relationships for C6 Substitutents at A$_1$ and A$_{2A}$ Adenosine Receptors. *Bioorg. Med. Chem.* **2000**, *8*, 2581−2590.

(9) van Galen, P. J. M.; Nissen, P.; van Wijngaarden, I.; IJzerman, A. P.; Soudijn, W. 1*H*-Imidazo[4,5-*c*]quinolin-4-amines: Novel Non-Xanthine Adenosine Antagonists. *J. Med. Chem.* **1991**, *34*, 1202−1206.

(10) Sarges, R.; Howard, H. R.; Browne, R. G.; Lebel, L. A.; Seymour, P. A.; Koe, B. K. 4-Amino[1,24]triazolo[4,3-*a*]quinoxalines. A Novel Class of Potent Adenosine Receptor Antagonists and Potential Rapid-Onset Antidepressants. *J. Med. Chem.* **1990**, *33*, 2240−2254.

(11) Muller, C. E. A$_1$ Adenosine Receptors and their Ligands: Overview and Recent Developments. *Farmaco* **2001**, *56*, 77−80.

(12) Hess, S. Recent Advances in Adenosine Receptor Antagonist Research. *Expert Opin. Ther. Pat.* **2001**, *11*, 1533−1561.

(13) van Muijlwijk-Koezen, J. E.; Timmerman, H.; Voelinga, R. C.; Frijtag von Drabbe Künzel, J.; de Groote, M.; Visser, S.; IJzerman, A. P. Thiazole and Thiadiazole Analogues as a Novel Class of Adenosine Receptor Antagonists. *J. Med. Chem.* **2001**, *44*, 749−762.

(14) van Tilburg, E. W.; van der Klein, P. A. M.; de Groote, M.; Beukers, M. W.; IJzerman, A. P. Substituted 4-Phenyl-2-(phenylcarboxamido)-1,3-thiazole Derivatives as Antagonists for the Adenosine A$_1$ Receptor. *Bioorg. Med. Chem. Lett.* **2001**, *11*, 2017−2019.

(15) Li, A.-H.; Moro, S.; Forsyth, N.; Melman, N.; Ji, X.-d; Jacobson, K. A. Synthesis, CoMFA Analysis, and Receptor Docking of 3,5-Diacyl-2,4-Dialkylpyridine Derivatives as Selective A$_3$ Adenosine Receptor Antagonists. *J. Med. Chem.* **1999**, *42*, 706−721.

(16) Li, A.-H.; Moro, S.; Melman, N.; Ji, X.-d.; Jacobson, K. A. Structure−Activity Relationships and Molecular Modeling of 3,5-Diacyl-2,4-dialkylpyridine Derivatives as Selctive A$_3$ Adenosine Receptor Antagonists. *J. Med. Chem.* **1998**, *41*, 3186−3201.

(17) van Rhee, M.; Jiang, J.-L.; Melman, N.; Olah, M. E.; Stiles, G. L.; et al. Interaction of 1,4-dihydropyridines and pyridine derivatives with adenosine receptors: selectivity for A$_3$ Receptors. *J. Med. Chem.* **1996**, *39*, 2980−2989.

(18) Bayer Aktiengesellschaft: WO0125210, 2001. Bayer Aktiengesellschaft: DE10115922A1, 2002.

(19) Beukers, M. W.; Chang, L. C. W.; von Frijtag Drabbe Künzel, J. K.; Mulder-Krieger, T.; Spanjersberg, R. F.; Brussee, J.; IJzerman, A. P. New, Non-Adenosine, High Potency Agonists for the Human Adenosine A$_{2B}$ Receptor with an Improved Selectivity Profile Compared to the Reference Agonist NECA. *J. Med. Chem.* **2004**, *47*, 3707−3709.

(20) Porkka-Heiskanenm, T.; Strecker, R. E.; Thakkar, M.; Bjørkum, A. A.; Greene, R. W.; McCarley, R. W. Adenosine: A Mediator of the Sleep-Inducing Effects of Prolonged Wakefulness. *Science* **1997**, *276*, 1265−1268.

(21) Porkka-Heiskanenm, T.; Alanko, L.; Kalinchuk, A.; Stenburg, D. Adenosine and Sleep. *Sleep Med. Rev.* **2002**, *6*, 321−332.

(22) Dunwiddle, T. V.; Masino, S. A. The Role and Regulation of Adenosine in the Central Nervous System. *Annu. Rev. Neurosci.* **2001**, *24*, 31−55.

(23) Clark, D. E. *In Silico* Prediction of Blood-Brain Barrier Permeation. *Drug Discovery Today* **2003**, *8*, 927−933.

(24) Norinder, U.; Haeberlein, M. Computational Approaches to the Prediction of the Blood-Brain Distribution. *Adv. Drug Delivery Rev.* **2002**, *54*, 291−313.

(25) Kelder, J.; Grootenhuis, P. D. J.; Bayada, D. M.; Delbressine, L. P. C.; Ploemen, J.-P. Polar Molecular Surface as a Dominating Determinant for Oral Absorption and Brain Penetration of Drugs. *Pharm. Res.* **1999**, *16*, 1514−1519.

(26) Oprea, T. I.; Gottfries, J. Toward Minimalistic Modeling of Oral Drug Absorption. *J. Mol. Graphics Modell.* **1999**, *17*, 261−274.

(27) Clark, D. E. Rapid Calculation of Polar Molecular Surface Area and Its Application to the Prediction of Transport Phenomena. 1. Prediction of Intestinal Absorption. *J. Pharm. Sci.* **1999**, *88*, 807−814.

(28) Clark, D. E. Rapid Calculation of Polar Molecular Surface Area and Its Application to the Prediction of Transport Phenomena. 2. Prediction of Blood-Brain Barrier Penetration. *J. Pharm. Sci.* **1999**, *88*, 815−821.

(29) Palm, K.; Luthman, K.; Ungell, A.-L.; Strandlund, G.; Artursson, P. Correlation of Drug Absorption with Molecular Surface Properties. *J. Pharm. Sci.* **1996**, *85*, 32−39.

(30) SPARTAN 5.0; Wavefunction, Inc., Irvine, CA92612; 1995.

(31) Da Settimo, F.; Primofiore, G.; Taliani, S.; Marini, A. M.; La Motta, C.; Novellino, E.; Greco, G.; Lavecchia, A.; Trincavelli, L.; Martini, C. 3-Aryl[1,2,4]triazino[4,3-a]benzimidazol-4(10H)-ones: A New Class of Selective A$_1$ Adenosine Receptor Antagonists. *J. Med. Chem.* **2001**, *44*, 316−327.

(32) Novellino, E.; Abignente, E.; Cosimelli, B.; Greco, G.; Iadanza, M.; Laneri, S.; Lavecchia, A.; Rimoli, M. G. Design, Synthesis and Biological Evaluation of Novel *N*-Alkyl- and *N*-Acyl-(7-substitued-2-phenylimidazo[1,2-*a*][1,3,5]triazin-4-yl)amines (ITAs) as Novel A$_1$ Adenosine Receptor Antagonists. *J. Med. Chem.* **2002**, *45*, 5030−5036.

(33) Bondavalli, F.; Botta, M.; Bruno, O.; Ciacci, A.; Corelli, F.; Fossa, P.; Lucacchini, A.; Manetti, F.; Martini, C.; Menozzi, G.; Mosti, L.; Ranise, A.; Schenone, S.; Tafi, A.; Trincavelli, M. L. Synthesis, Molecular Modeling Studies, and Pharmacological Activity of Selective A$_1$ Receptor Antagonists. *J. Med. Chem.* **2002**, *45*, 4875−4887.

(34) Lipinski, C. A.; Lombardo, F.; Dominy, B. W.; Feeney, P. J. Experimental and Computational Approaches to Estimate Solubility and Permeability in Drug Discovery and Development Settings. *Adv. Drug Delivery Rev.* **1997**, *23*, 3−25.

(35) de Valk, J.; van der Plas, H. C. On the Mechanism of the Amination of 4-Bromo-2,6-Diphenyl- and 4,5-Dibromo-2,6-diphenyl-pyrimidine. *Receuil* **1973**, *92*, 145−155.

(36) Brown, D. J.; Cowden, W. B.; Lan, S.-B.; Mori, K. Heterocyclic Amplifiers of Phleomycin. I. Some Pyrimidinylpurines, Pyrimidinylpteridines and Phenylpyrimidines. *Aust. J. Chem.* **1984**, *37*, 155−163.

(37) Al-Hajjar, F. H.; Sabri, S. S. Reaction of α,β-Unsaturated Ketones with Guanidine. Substituent Effects on the Protonation Constants of 2-Amino-4,6-diarylpyrimidines. *J. Heterocycl. Chem.* **1982**, *19*, 1087−1092.

(38) van Muijlwijk-Koezen, J. E.; Timmerman, H.; Link, R.; van der Groot, H.; IJzerman, A. P. A Novel Class of Adenosine A$_3$ Receptor Ligands. Structure Affinity Profile of a Series of Isoquinoline and Quinazoline Compounds. *J. Med. Chem.* **1998**, *41*, 3994−4000.

(39) Topliss, J. G. Utilization of Operational Schemes for Analog Synthesis in Drug Design. *J. Med. Chem.* **1972**, *15*, 1006−1011.

(40) Ceccarelli, S.; D'Alessandro, A.; Prinzivalli, M.; Zanarella, S. Imidazo[1,2-*a*]quinozalin-4-amines: A Novel Class of Nonxanthine A$_1$ Adenosine Receptor Antagonists. *Eur. J. Med. Chem.* **1998**, *33*, 943−955.

(41) Trivedi, B. K.; Bruns, R. F. [1,2,4]Triazolo[4,3-*a*]quinoxalin-4-amines: A New Class of A$_1$ Receptor Selective Adenosine Antagonists. *J. Med.Chem.* **1988**, *31*, 1011−1014.

(42) Volpini, R.; Costanzi, S.; Vittori, S.; Cristalli, G.; Klotz, K.-N. Medicinal Chemistry and Pharmacology of A$_{2B}$ Adensoine Receptors. *Curr. Top. Med. Chem.* **2003**, *3*, 427−443.

(43) van Muilwijk-Koezen, J. E.; Timmerman, H.; van der Goot, H.; Menge, W. M. P. B.; Frijtag von Drabbe Künzel, J.; de Groote, M.; IJzerman, A. P. Isoquinoline and Quinazoline Urea Analogues as Antagonists for the Human Adenosine A$_3$ Receptor. *J. Med. Chem.* **2000**, *43*, 2227−2238.

(44) Schingnitz, G.; Küfner-Mühl, U.; Ensinger, H.; Lehr, E.; Kuhn, F. J. Selective A$_1$-Antagonists for Treatment of Cognitive Deficits. *Nucleosides Nucleotides* **1991**, *10*, 1067−1076.

(45) Baddar, F. G.; Al-Hajjar, F. H.; El-Rayyes, N. R. Acetylinic Ketones. Part II. (Ia). Reaction of Acetylenic Ketones with Nucleophilic Nitrogen Compounds. *J. Heterocycl. Chem.* **1976**, *13*, 257−268.

(46) Campbell, R. M.; Cartwright, C.; Chen, W.; Chen, Y.; Duzic, E.; Fu, J.-M.; Loveland, M.; Manning, R.; McKibben, B.; Pleiman, C. M.; Silverman, L.; Trueheart, J.; Webb, D. R.; Wilinson, V.; Witter, D. J.; Xie, X.; Castelhano, A. L. Selective A$_1$ Adenosine Receptor Antagonists Identified Using Yeast *Sacchacromyces Cerevisiae* Functional Assays. *Bioorg. Med. Chem. Lett.* **1999**, *9*, 2413−2418.

(47) Francis, J. E.; Cash, W. D.; Psychoyos, S.; Ghai, G.; Wenk, P.; Friedmann, R. C.; Atkins, C.; Warren, V.; Furness, P.; Hyun, J. L.; Stone, G. A.; Desai, M.; Williams, M. Structure−Activity Profile of a Series of Novel Triazoloquinazoline Adenosine Antagonists *J. Med. Chem.* **1988**, *31*, 1014−1020.

(48) Klotz, K.-N.; Hessling, J.; Hegler, J.; Owman, C.; Kull, B.; Fredholm, B. B.; Lohse, M. J. Comparative Pharmacology of Human Adenosine Receptor Subtypes−Characterization of Stably Transfected Receptors in CHO cells. *Naunyn-Schmiedeberg's Arch. Pharmacol.* **1998**, *357*, 1−9.